

# Numerical Study on Ship Motion Coupled with LNG tank Sloshing Using Dynamic Overset Grid Approach

\*Y. Zhuang, C.H. Yin and †D.C. Wan

State Key Laboratory of Ocean Engineering, School of Naval Architecture, Ocean and Civil Engineering,  
Shanghai Jiao Tong University, Collaborative Innovation Center for Advanced Ship and Deep-Sea Exploration,  
Shanghai 200240, China

\* Presenting author: nana2\_0@sjtu.edu.cn.

†Corresponding author: dcwan@sjtu.edu.cn.

## Abstract

In this paper, numerical simulations of ship motion coupled with LNG tank sloshing in waves are considered. The fully coupled problems are performed by our in-house RANS/DES solver, naoe-FOAM-SJTU, which is developed based on the open source tool libraries of OpenFOAM. The internal tank sloshing and external wave flow are solved simultaneously. The considered models are LNG FPSO and a modified KVLCC2 coupled with two LNG tanks respectively. Three degrees of freedom is released in the regular waves. The ship motion responses of LNG FPSO are carried out both in head and beam waves to compare with existing experimental data to validate this solver. Next, the modified KVLCC2 coupled with two LNG tanks and a propeller is simulated with a forward-speed in the head wave using dynamic overset method. Two filling ratios of tanks: 30% and 60% are considered, and results are compared with that without sloshing.

**Keywords:** LNG sloshing, OpenFOAM, nonlinear coupled motion, dynamic overset grids, naoe-FOAM-SJTU solver

## Introduction

The sailing performance of the ship equipped with liquid tanks is different from that without tanks. The sloshing flow in tanks which is excited by ship motion would affect ship performance in return. This coupling effect not only causes impact pressure which may damage the cargo, but also changes ship motion in waves. It is especially essential for FLNG or FPSO, for these kinds of vessels suffer from both external wave force and internal force when they transport liquid cargoes on the sea. Therefore, the maneuvering of ship equipped with liquid cargoes in waves is still a researchable issue. Since the coupling effect is nonlinear and viscosity in sloshing flow is ignorable, the numerical simulation has its advantages to treat this problem. Computational Fluid Dynamics (CFD) is an effective method to simulate the ship motion in waves coupled with LNG tank sloshing, and with the assistant of overset grid technology, the coupling effect of large-amplitude motion such as self-propulsion in waves with partially filled tanks can be solved effectively.

Several researches about ship motion coupled with tank sloshing have been done. Nam, B.W. et al[1] carried out both numerical and experimental studies of LNG FPSO model. The

impulse-response-function (IRF) was used to simulate ship motion and finite-difference method was adopted to solve nonlinear tank sloshing. In recent decades, many studies used viscous flow theory in order to solve the nonlinearity of the tank sloshing. Li, Y. L. et al[2] applied both potential flow theory and viscous flow theory under OpenFOAM. Jiang, S. C. et al[3] also used OpenFOAM to simulate the coupling effect, and applied VOF to capture the interface, and the paper still considered ship response in IRF method. Shen, Z. R. et al[4] achieved fully coupled of ship motion and tank sloshing by the unsteady RANS solver, naoe-FOAM-SJTU. Considering the ship performance with sloshing tanks at forward speed in the sea, Kim, B. et al[5] studied the coupled seakeeping and sloshing tanks in frequency domain. A forward-speed seakeeping theory was implemented to investigate the coupling effects. Mitra, S. et al[6] investigated the coupling effect in six degrees of freedom, solving the sloshing tank in potential flow equation and finite element method. The hybrid marine control system was applied to simulate the maneuvering of the ship.

In this paper, ship motion coupled with LNG tanks is simulated by CFD method. The internal sloshing tank and external sea waves are treated as an entire computational region, and both solved by RANS solver simultaneously. The Volume of fluid (VOF) method is applied to capture both outside wave surface and sloshing liquid. The computations are solved by our in house solver naoe-FOAM-SJTU with dynamic overset grid capability[7]. SUGGAR++ is used to obtain DCI[8], which connects the information of overset component grids. The solver contains 6DOF module, wave generation and damping module for various wave types.

To validate the current CFD method, five different filling ratios of LNG FPSO with two tanks in waves are selected. The simulation is compared with existing experimental results to prove the ability of our solver. To observe the coupling effect on large-amplitude motion, a benchmark ship KVLCC2 equipped with two LNG tanks and propeller is also considered. The simulation conditions include three different filling ratios (0%, 30% and 60%) in head waves with forward-speed.

## Numerical Methods

The incompressible Reynolds-Averaged Navier-Stocks equations are adopted in this paper to investigate the viscous flow. The governing equations are:

$$\nabla \cdot \mathbf{U} = 0 \quad (1)$$

$$\frac{\partial \rho \mathbf{U}}{\partial t} + \nabla \cdot (\rho(\mathbf{U} - \mathbf{U}_g)\mathbf{U}) = -\nabla p_d - \mathbf{g} \cdot \mathbf{x} \nabla \rho + \nabla \cdot (\mu_{eff} \nabla \mathbf{U}) + (\nabla \mathbf{U}) \cdot \nabla \mu_{eff} + f_\sigma + f_s \quad (2)$$

Where  $\mathbf{U}$  is velocity field,  $\mathbf{U}_g$  is velocity of grid nodes;  $p_d = p - \rho \mathbf{g} \cdot \mathbf{x}$  is dynamic pressure;

$\mu_{eff} = \rho(\nu + \nu_t)$  is effective dynamic viscosity, in which  $\nu$  and  $\nu_t$  are kinematic viscosity and eddy viscosity respectively.  $f_\sigma$  is the surface tension term in two phases model. The

solution of momentum and continuity equations is implemented by using the pressure-implicit split operator (PISO) algorithm. A  $k-\omega$  SST model is selected for turbulence closure[9].

The Volume of fluid (VOF) method with bounded compression techniques is applied to control numerical diffusion and capture the two-phase interface efficiently. The VOF transport equation is described below:

$$\frac{\partial \alpha}{\partial t} + \nabla \cdot [(\mathbf{U} - \mathbf{U}_g)\alpha] + \nabla \cdot [\mathbf{U}_r(1-\alpha)\alpha] = 0 \quad \phi_I = \sum_{i=1}^n \omega_i \cdot \phi_i \quad (3)$$

Where  $\alpha$  is volume of fraction, indicating the relative proportion of fluid in each cell and its value is always between zero and one:

$$\begin{cases} \alpha = 0 & \text{air} \\ \alpha = 1 & \text{water} \\ 0 < \alpha < 1 & \text{interface} \end{cases} \quad (4)$$

The overset grid technique is implemented into OpenFOAM to handle the large-amplitude motion of ship and complex hierarchical motion of appendages such as rotating propeller and moving rudder[10]. The overset grid method allows separate overlapping grids to move independently without restrictions. The hole cells located outside the domain or of no interest, such as inside a body, are excluded from computation. The cells around hole cells are marked as fringe or receptor cells, they receive the information from other component grids by interpolation. Donor cells provide information to the fringe cell from donor grid. The value for fringe cell is obtained by the summation of weight coefficients and the values of donor cells

$$\phi_I = \sum_{i=1}^n \omega_i \cdot \phi_i \quad (5)$$

Where  $\omega_i$  are the weight coefficients and  $\phi_i$  is the value of donor cell;  $\phi_I$  is the resulting value in the interpolated fringe cell;  $n$  is the number of donor cells and it is equal to eight if the structured grid is employed. And then the values of fringe cells need update with interpolated ones. The suitable approach for implicit scheme is to modify the matrix in the linear algebraic system after discretizing the equations

A fully 6DOF module with hierarchy of bodies are implemented. This module allows ship to move independently in the computational domain and in the meanwhile, the propeller is rotating around the propeller axis. Two coordinate systems, earth-fixed and ship-fixed systems are adopted in this 6DOF module. The forces and moments on ship hull and propeller are computed in earth-fixed system and then they are projected to ship-fixed system. The ship motions for the next time step are predicted by the projected forces and moments in ship fixed

system. For the movements of hierachal objects, the propeller grid rotates first about a fixed axis in the ship coordinate system, and then both ship and propeller grids translate and rotate in the earth-fixed system according to the predicted motions, as shown in Fig.1. In the meanwhile, SUGGAR++ library is called to compute the DCI based on the new grid positions. OpenFOAM processors receive the new data right after the movements of the overset grids and start the computation for the next time step. For the details of the implementations of overset capability and 6DOF module can be referred to [8].

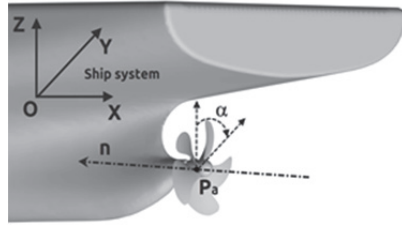


**Fig.1 Demonstration of propeller rotating in the ship system**

The incoming regular wave is generated by imposing the boundary conditions of  $\alpha$  and  $\mathbf{U}$  at the inlet. The linear Stokes wave in deep water is applied for the wave generation.

$$\xi(x, t) = a \cos[k(x - x_{cg}) - \omega_e t] \quad (6)$$

$$u(x, y, z, t) = U_0 + a\omega e^{kz} \cos[k(x - x_{cg}) - \omega_e t] \quad (7)$$

$$w(x, y, z, t) = a\omega e^{kz} \sin[k(x - x_{cg}) - \omega_e t] \quad (8)$$

Where  $\xi$  is the wave elevation;  $a$  is the wave amplitude;  $k$  is the wave number;  $U_0$  is the ship velocity;  $\omega$  is the natural frequency of wave;  $\omega_e$  is the encounter frequency, given by  $\omega_e = \omega_e + kU_0$  in head waves;  $x_{cg}$  is the longitudinal gravity center of the ship model, it is used to adjust the phase of the incident wave to make the wave crest reach the gravity center of ship at  $t = 0$ .

## Validation

### Geometry and Condition

To validate the current method, a LNG FPSO model with two prismatic tanks is selected. The main particulars of LNG FPSO are shown in Table 1. To compare with experiments which have been done by Nam, B. W. et al[1], the LNG FPSO model is 1/100 scale of the full scale ship. The length, breadth and height of the fore tank and the aft tank are 49.68m, 46.92m, 32.23m and 56.62m, 46.92m, 32.23m respectively. The distance from the bottom of tank to

the keel line is 3.3m. The geometry of experimental ship model and numerical ship model are illustrated in Fig 3.

Five different filling conditions and two wave directions are included to verify the computations. The settings of numerical computation for head wave and beam wave are illustrated in Fig.2. To compare with experiment data, the filling ratios carried out as the same with those in experiments: 0%-0% (fore tank-aft tank), 20%-20%, 30%-30%, 57.5%-43.3% and 82.6%-23.5%. Those filling conditions are shown in Fig 4. The daft at each condition were kept the same, as well as longitudinal moment inertia.

**Table 1 Main particular of LNG FPSO**

Main particulars		Full Scale	Model
Scale factor	—	1	1/100
Length between perpendiculars	L <sub>PP</sub> (m)	285	2.85
Maximum beam of waterline	B <sub>WL</sub> (m)	63	0.63
Draft	T (m)	13	0.13
Displacement	$\Delta$ (m <sup>3</sup> )	220017.6	220.0176
Natural period of roll	T <sub>θ</sub> (s)	13	1.3
Vertical Center of Gravity (from keel)	K <sub>G</sub> (m)	16.5	0.165
Radius of gyration	K <sub>xx</sub>	19.45	0.1945
	K <sub>yy</sub>	71.25	0.7125

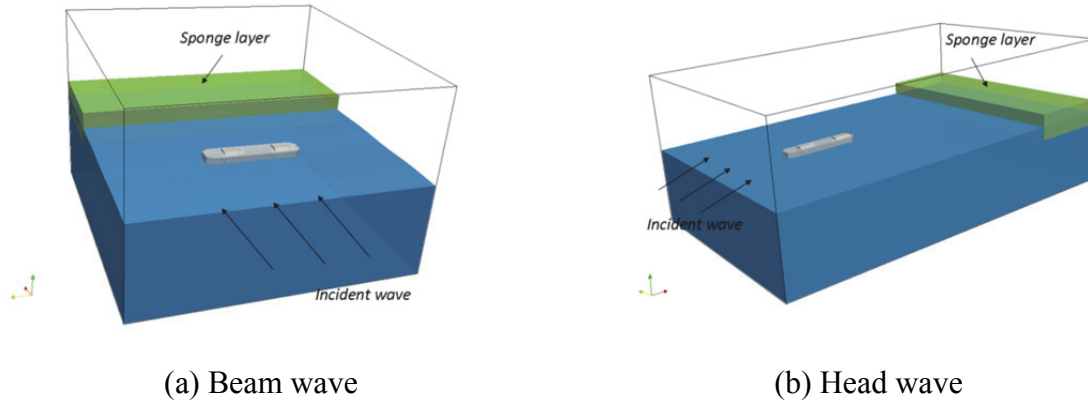


**Fig.2 Setup of numerical computation**

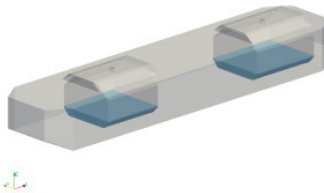


(a) Experimental ship model

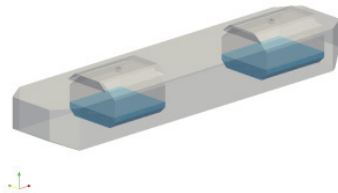


(b) Numerical simulation model

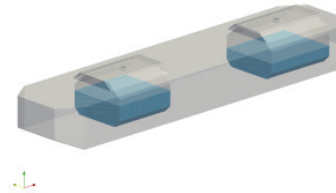
**Fig. 3 geometry of LNG FPSO**



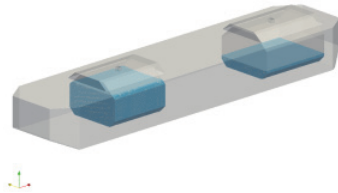
(a) 20%~20%



(b) 30%~30%



(c) 57.5%~43.3%



(d) 82.6%~23.5%

**Fig. 4 filling ratios of LNG FPSO equipped with LNG tanks**

Considering the large-amplitude motion of LNG FPSO, the length of regular wave is chosen as 2.865m, 1.005 times length of the ship. Same to the experiment, the wave height is fixed to 0.025m, and encounter frequency is 4.6382.

#### Mesh

There are two computational domain in beam wave condition and head wave condition. The selected domain is described as  $-1.0L_{pp} < x < 2.0L_{pp}$ ,  $-1.5L_{pp} < y < 1.5L_{pp}$ ,  $-1.0L_{pp} < z < 1.0L_{pp}$  in beam wave condition; and  $-2.0L_{pp} < x < 4.0L_{pp}$ ,  $-1.5L_{pp} < y < 1.5L_{pp}$ ,  $-1.0L_{pp} < z < 1.0L_{pp}$  in head wave condition. The meshes are generated by *snappyHexMesh*, an auto mesh generation utility provided by OpenFOAM. The total cell numbers are around 2.1M, and the LNG tanks require additional 0.5M cells. The mesh details are shown in Fig. 5. Two small tunnels are used to connect the LNG tanks to the external region, which can keep the pressure inside the tanks same to the external region, and simplify the computations.

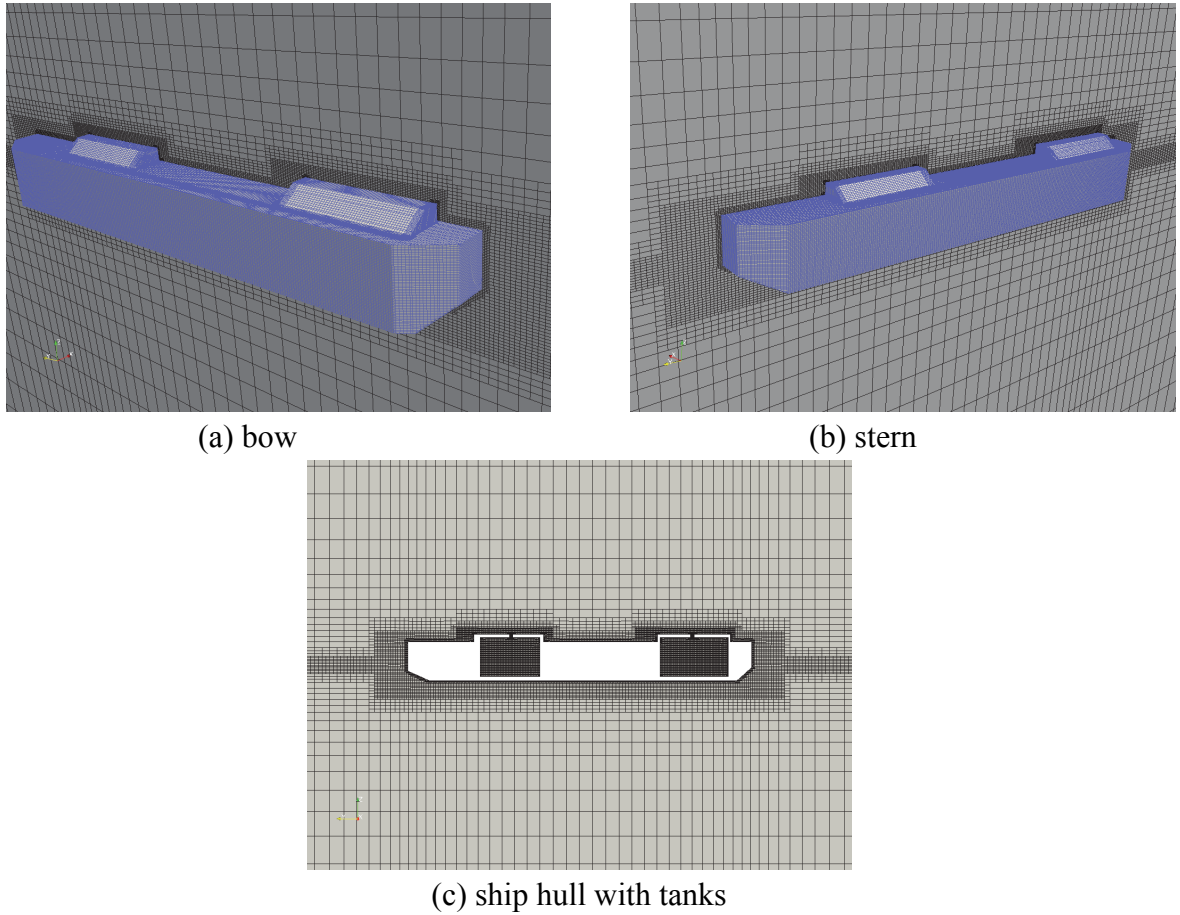


**Fig.5 Demonstrations of meshes**

### Results

The ship motion was restricted to three degree-of-freedom, heave, pitch and roll. Beam wave conditions are analyzed first. Time histories of heave and roll motion are shown in Fig.6. The normalized motion amplitude and natural frequency were considered to compare with experimental data. The normalized roll motion is given as:  $R_1 = \theta B / 2A$ , which  $\theta$  is maximum degree of roll motion, B is beam of ship and A is wave amplitude; The normalized heave motion is given as:  $H_1 = \xi / A$ , which  $\xi$  is the maximum value of heave motion; and normalized natural frequency is given as:  $T = \omega(L/g)^{1/2}$ , which  $\omega$  is natural frequency of water, L represents length of ship. Computations in this paper uses T=2.5 when the wave length is close to ship length.

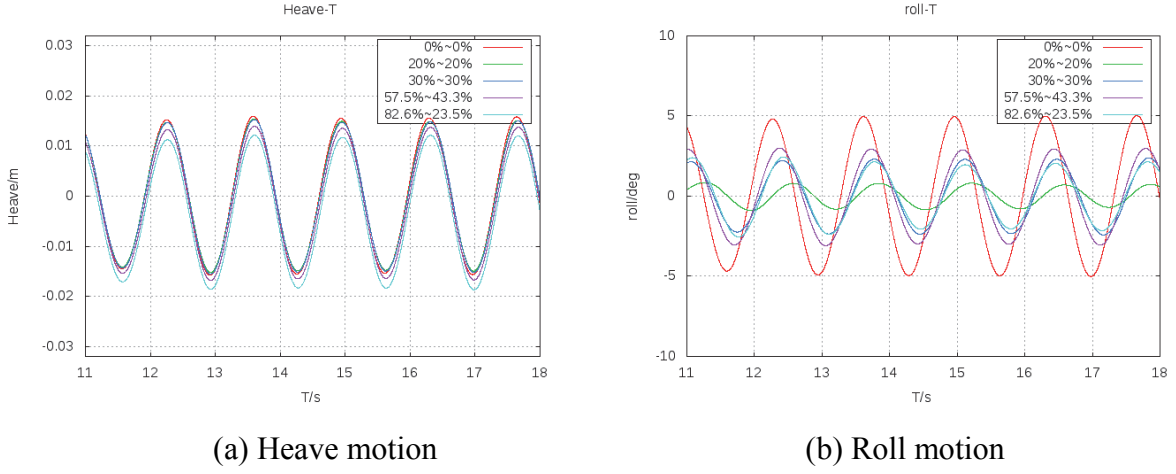
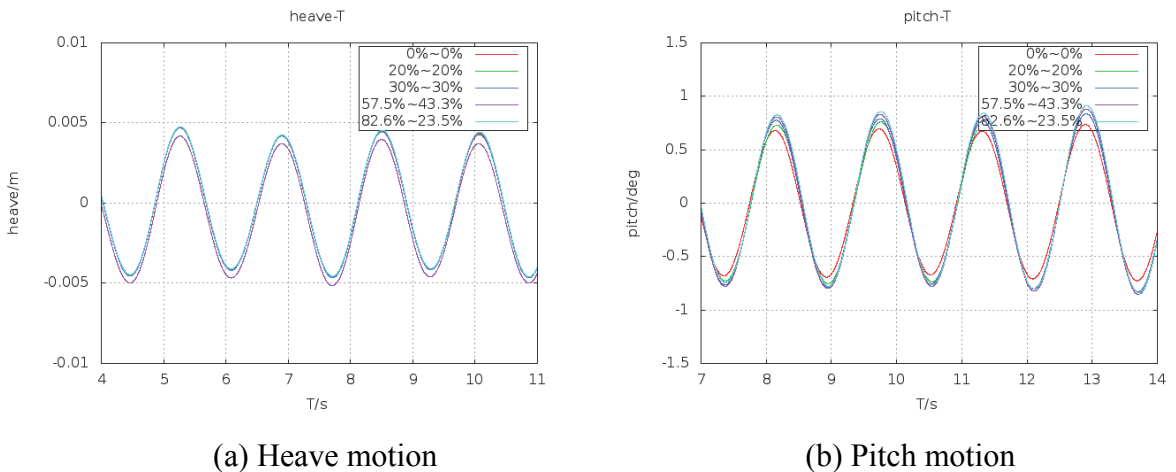


**Fig6. Time history of heave and roll motion with different filling ratios in beam wave**

**Table 2 Comparison of ship motion between CFD and experiments in beam wave**

No	Filling ratio	EFD( $R_1$ )	CFD( $R_1$ )	EFD( $H_1$ )	CFD( $H_1$ )
1	0%~0%	1.85	2.00(8%)	1.25	1.28(2.4%)
2	20%~20%	0.60	0.53(-12%)	-	1.22
3	30%~30%	1.25	1.12(-10%)	-	1.21
4	57.5%~43.3%	1.30	1.28(-1.5%)	-	1.10
5	82.6%~23.5%	1.20	1.10(-8.3%)	-	1.04

Table 2 shows the comparison of roll motion and heave motion between current computation and experiments in beam waves. Five different filling conditions were considered, and the results fairly agree with those in experiments. The head wave conditions were also selected to validate the method in head waves. Fig.7 illustrates the time history of heave and pitch motion.



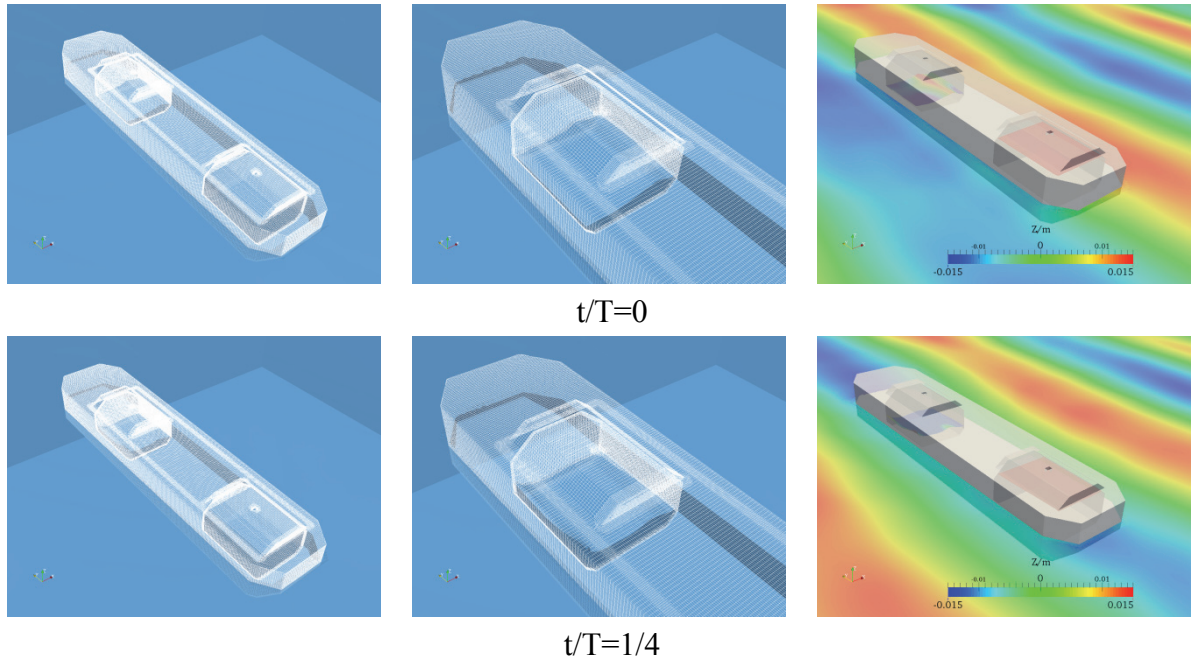
**Fig7. Time history of heave and pitch motion with different filling ratios in head wave**

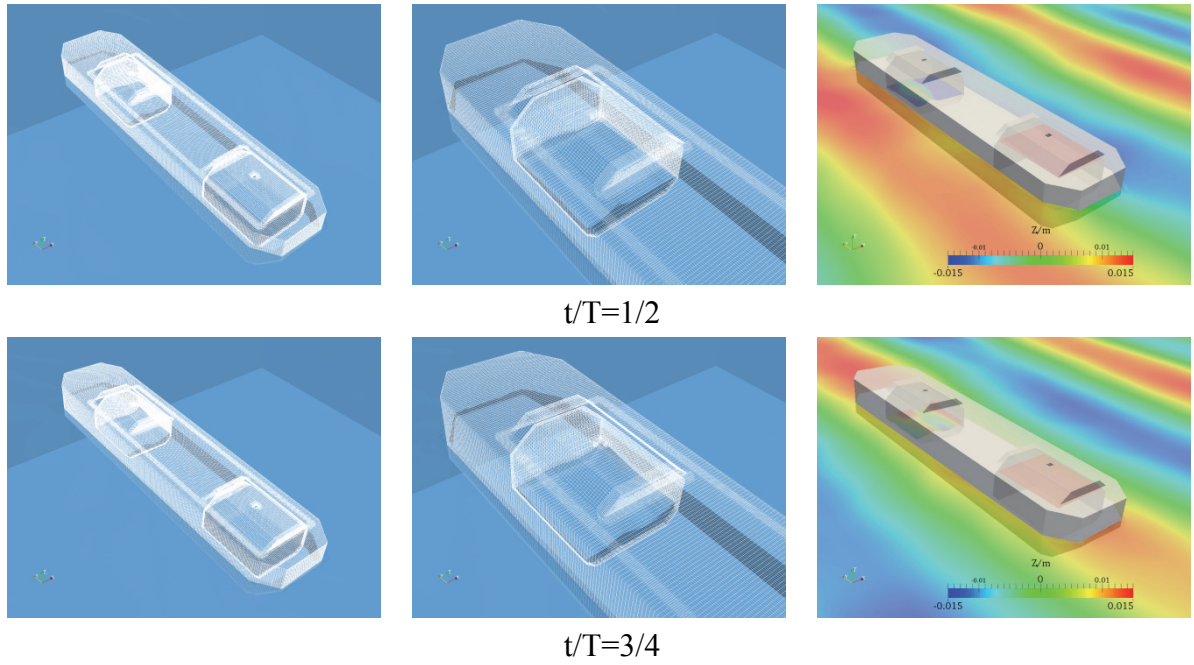
Table 3 shows the results comparison between current simulation and experimental results. The dimensionless parameters of ship motion are considered. The normalized pitch motion is given as:  $P_1 = \theta L / 2A$ , which  $L$  is ship length. Five filling conditions were considered and compared to the existing experimental data, the simulation results fairly agree with the experimental results.

**Table 3 Comparison of ship motion between CFD and experiments in head wave**

No	Filling ratio	EFD( $\mathbf{P}_1$ )	CFD( $\mathbf{P}_1$ )	EFD( $\mathbf{H}_1$ )	CFD( $\mathbf{H}_1$ )
1	0%~0%	1.20	1.31(9.3%)	0.12	0.14(16%)
2	20%~20%	1.13	1.30(15%)	-	0.14
3	30%~30%	1.30	1.45(11%)	0.12	0.14(16%)
4	57.5%~43.3%	-	1.60	-	0.138
5	82.6%~23.5%	-	1.63	-	0.14

Fig.6 and Fig.7 indicates that the ship exhibits sinusoidal motion both in head and beam waves. The coupling effects are limited in head wave. In beam wave condition, the coupling effects of ship motion and tank sloshing are not obvious in heave motion, shown in Fig.6(a), but quite significant in roll motion, shown in Fig.6(b). The four partially filling conditions of sloshing tanks all reduce the roll amplitude of ship motion; on the contrary, although not obvious in head waves, the filling conditions increase the amplitude of ship motion. In beam wave, for low-filling condition, like 20%~20%, the decrease in amplitude of roll motion is evident and thus shows great coupling effect. For the water in tanks is shallow, the sloshing in tanks is more violent and influence ship motion more.





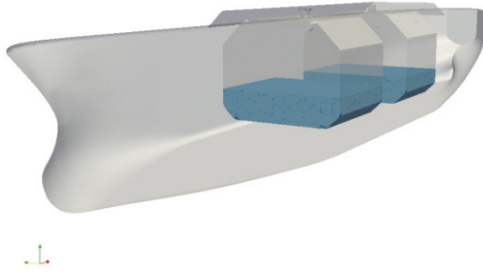
**Fig.8 Four snapshots of LNG FPSO motion in beam regular waves. From left to right: global view, detail view of the aft tank sloshing and view of free surface in turn. 82.6%~23.5% filled, wave propagates from left to right.**

Fig.8 illustrates four snapshots of ship motion coupled with 82.6%-23.5% filling ratio in one period (1.35s), wave propagates from left to right. The fore tank has insignificant coupling effects, so the aft tank is studied in details. The flow in aft tank shows different phase to that of ship motion. In the time  $t/T=0$ , ship stays in balance position, the sloshing liquid in aft tank starts to move from right to left. At  $t/T=1/4$ , the ship is in the region of wave trough, and begins to roll to the left (towards the wave direction); the peak of the tank liquid reaches the left bulkhead. At  $t/T=1/2$ , the ship returns to the balance position, the peak of the sloshing liquid moves to the right. At  $t/T=3/4$ , the wave crest reaches the ship and ship begins roll to the right, the peak of the in-tank flow arrives at the right bulkhead.

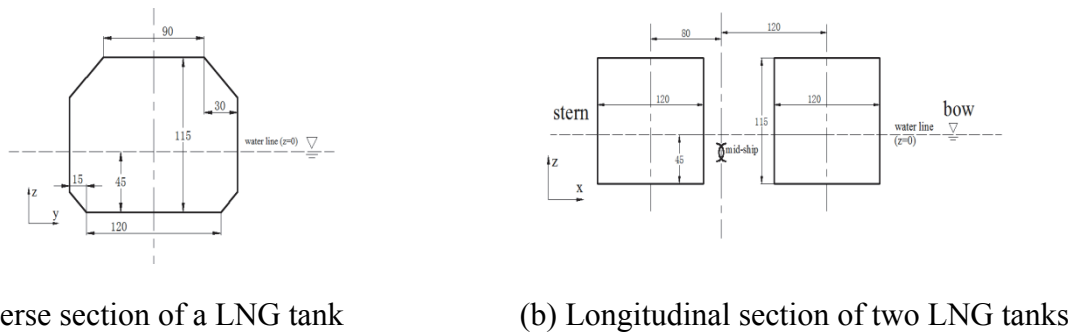
### Coupling Effects on KVLCC2 with a Propeller

#### *Geometry and Conditions*

To figure out the coupling effects on large-amplitude motion, KVLCC2, a benchmark ship in Gothenburg Workshop 2010 (G2010)[11] equipped with two LNG tanks and a propeller is considered. Fig.9 shows geometry of the ship and its LNG tanks and Table 4 illustrates the principle dimensions of KVLCC2. The modified KVLCC2 equipped with two identical LNG tanks, and the main particulars and settings of those tanks are shown in Fig. 10. The tanks are in model scale, and all the numbers are in mm.



**Fig.9 Geometry of KVLCC2 with two LNG tanks**



(a) Transverse section of a LNG tank

(b) Longitudinal section of two LNG tanks

**Fig. 10 Geometry of LNG tanks**

**Table 4 Main dimensions of KVLCC2**

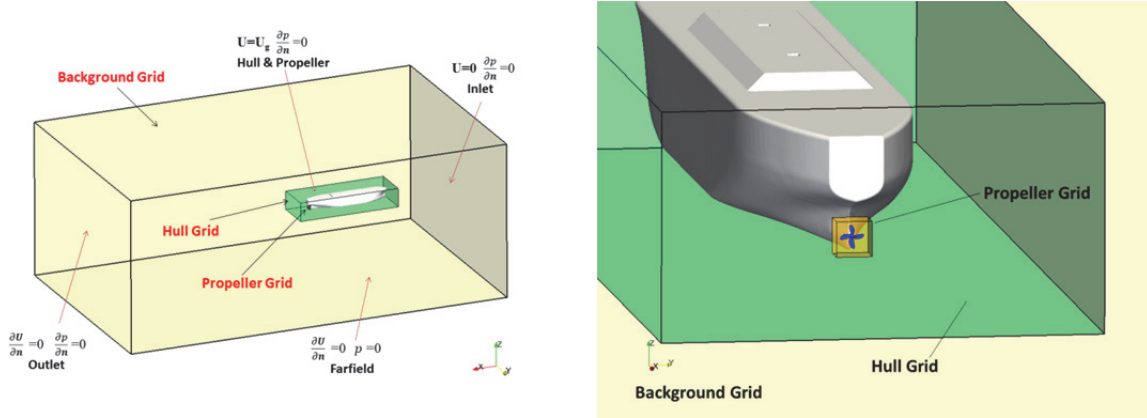
Main particulars		Full Scale	Model
Length between perpendiculars	$L_{pp}$ (m)	320	3.200
Maximum beam of waterline	$B_{WL}$ (m)	58	0.580
Depth	D (m)	30	0.300
Draft	T (m)	20.8	0.208
Displacement	$\Delta$ ( $m^3$ )	312622	0.313
Wetted area	$SW$ ( $m^2$ )	27194	2.719
Vertical Center of Gravity (from keel)	KG (m)	18.6	0.186
Moment of Inertia	$K_{xx}/B$	0.4	0.400
	$K_{yy}/L_{pp}, K_{zz}/L_{pp}$	0.25	0.250

To evaluate the coupling effects on self-propulsion, KVLCC2 with a certain velocity in head wave is calculated. The motions are allowed for roll, heave and pitch. Three different filling ratios are considered, 30%, 60% and no sloshing, respectively. The wave length is equal to 3.2m, and wave height is 0.12m. The ship has a forward-speed of  $Fr=0.179$ .

#### *Mesh and Computational Domain*

The space coordinate range of computational domain is  $-1.0L_{pp} < x < 4.0L_{pp}$ ,  $-1.5L_{pp} < y < 1.5L_{pp}$ ,  $-1.0L_{pp} < z < 1.0L_{pp}$ . The mesh is generated by automatic mesh generation tool *snappyHexMesh*. The overset grids consist of hull, background and propeller grids. The computational domain

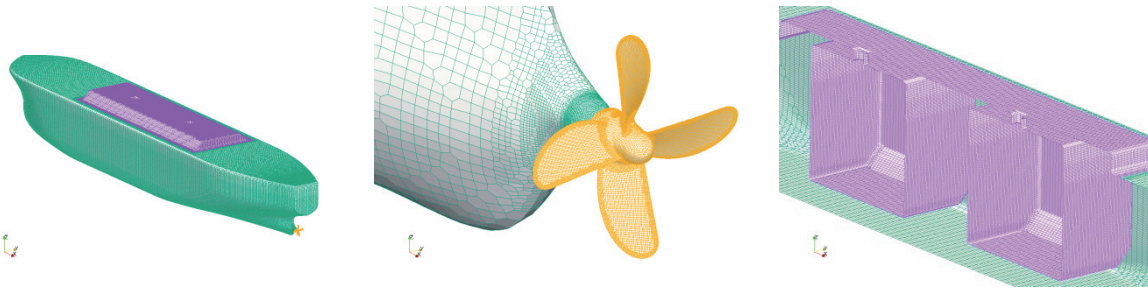
contains around 3.9M grid cells, in which hull uses 2.65M grid cells and propeller possesses 0.68M grid cells. Some regions have been refined to capture free surface, violent flow and vortex structure. Boundary conditions and layout of overset grid systems are displayed in Fig. 11, and the surface mesh of hull, tanks and propeller are shown in Fig. 12.



(a) Overall view

(b) Stern view

**Fig. 11 Layout of overset grid system**



(a) Hull mesh

(b) Propeller mesh

(c) Tank mesh

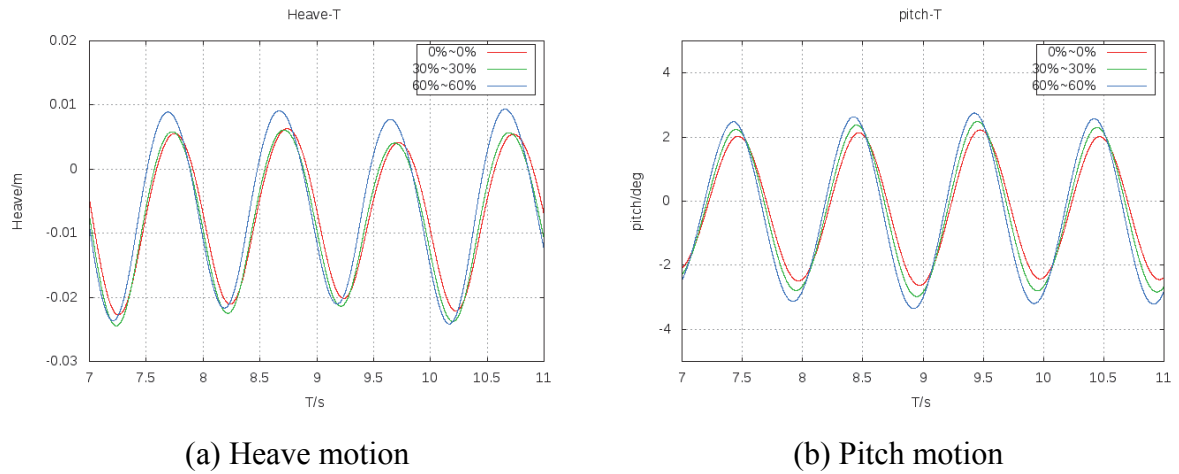
**Fig. 12 Mesh generation**

### Results

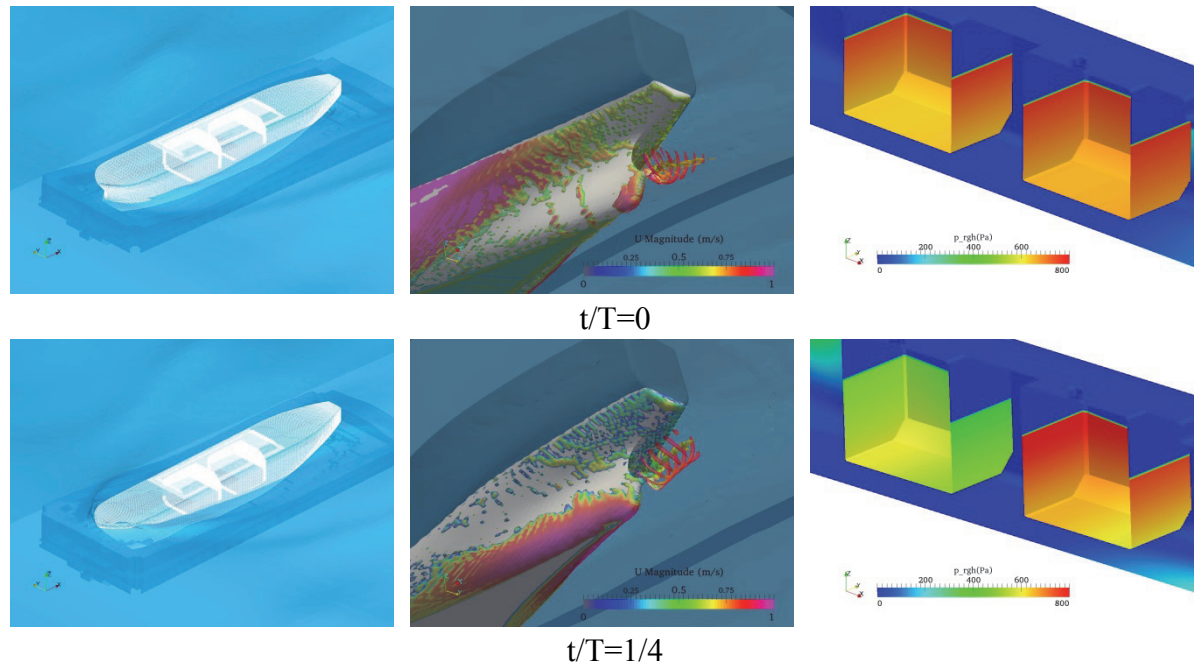
The pitch and heave motion of ship with a forward-speed in head wave are shown in Fig.13. Two different filling conditions are considered and compared to that without sloshing. The coupling effects are observed in pitch and heave motion but they are not prominent. The 60% filled ship has more violent motion than ship with 30% filling ratio and without sloshing.

Fig.14 illustrates four snapshots of ship motion and the dynamic pressure on bulkhead with 60% filling ratio in an encounter period. Propeller vortices behind ship stern are illustrated by iso-surfaces of  $Q=100$ . The iso-surfaces are colored by velocity magnitude. At  $t/T=0$ , ship stays at balanced position, the dynamic pressure on bulkhead stays the same in fore and aft tank. The value of dynamic pressure near in-tank liquid surface is larger than that near bottom bulkhead, which means liquid slosh more violent near surface. At  $t/T=1/4$ , the wave crest reaches and ship bow nearly buries into wave. The dynamic pressure on bulkhead decreases in fore tank and it increases in aft tank. At  $t/T=0$  and  $1/4$ , the velocity of propeller vortices is high, for the ship stern is near the surface, the load on the propeller blades is small

correspondingly. At  $t/T=1/2$ , ship returns back to balanced position, and the dynamic pressure on bulkhead stays the same in fore and aft tank. However, the dynamic pressure at this time is smaller than that at  $t/T=0$  and tank liquid slosh more violent near bottom than that near in-tank water surface. At  $t/T=3/4$ , the trough of wave reaches and ship bow nearly comes out of the surface. The dynamic pressure on bulkhead decreases in aft tank while it increases in fore tank. The tank liquid is not affected by ship motion intensively, for the surface in tanks slosh slight. Moreover, the dynamic pressure on bulkhead in fore and aft tank shows phase difference in an encounter period. At  $t/T=1/2$  and  $3/4$ , the ship stern buries into water, thus the loads on the propeller blades increase, and the velocity of propeller vortices is lower than that at  $t/T=0$  and  $1/4$ .



**Fig.13 Time history of heave and pitch motion at forward speed with different filling ratios in head wave.**



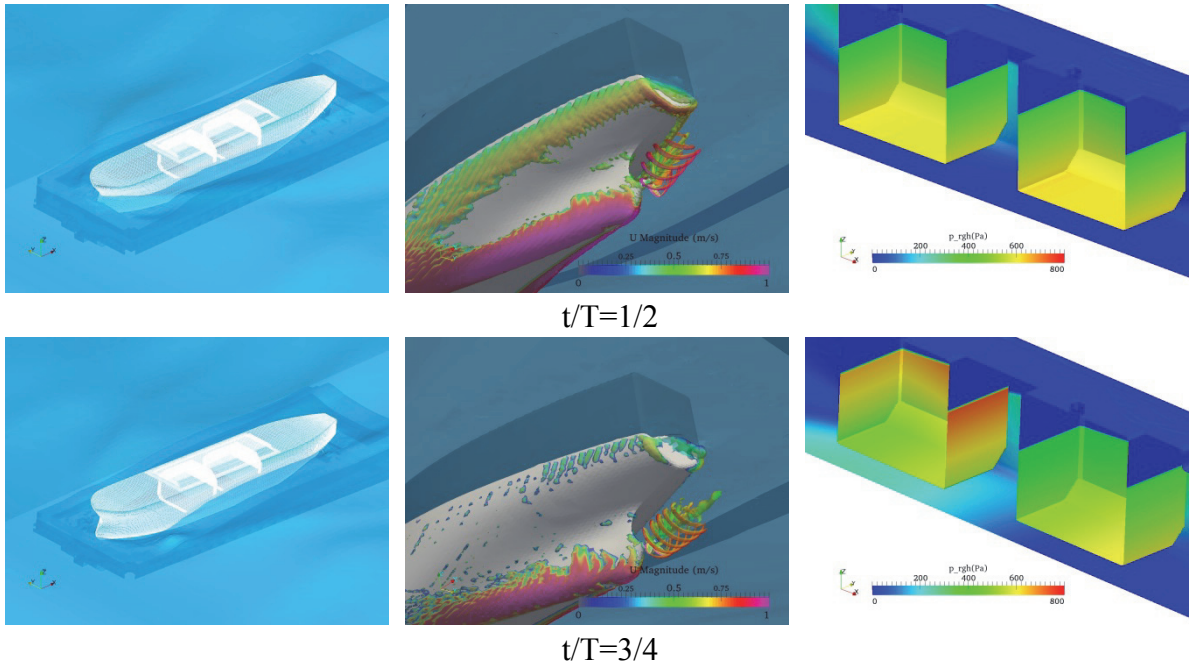


**Fig. 14 Snapshots of ship motion, Q iso-surfaces and dynamic pressure on bulkhead in one period**

## Conclusion

In this paper, the large-amplitude of ship motion fully coupled with internal sloshing tanks is studied. The numerical simulations are performed by the solver naoe-FOAM-SJTU, which is developed based on open source CFD package OpenFOAM and implemented with dynamic overset grid technique. The internal tank sloshing and external wave excitation are computed simultaneously by solving RANS equations. Two phase interface is captured by VOF method. To validate the current method, LNG FPSO is chosen to compare with existing measurements data. Five different filling conditions are considered both in the head and beam wave. The results show fairly agreement with those in experiments. At the meantime, the coupling effects are investigated. With the wave length equal to 1.005 times ship length, the sloshing has little effect on the heave and pitch motion both in the head and beam wave. However, the sloshing has remarkable effect on roll motion in the beam wave condition. The comparison between four different filling ratios with non-filling ratio indicates that all these four kinds of sloshing reduce the roll amplitude of ship motions, especially the low filling ratios, like 20% filled tanks.

To make a further study of large-amplitude ship motion coupled with sloshing tanks with a forward-speed in head waves, a KVLCC2 model equipped with two LNG tanks and a propeller is chosen. In the condition of wave length equal to ship length, two filling ratios are considered to compare with non-filling ratio condition in head wave. With the forward speed, the coupling effect can be observed but it is not obvious. Unlike coupling effect on roll motion in the beam wave, the tank sloshing increase the amplitude motion both in heave and pitch motion, especially for the 60% filled tanks.

However, in this stage, only one wave condition is considered in the simulation, thus more wave conditions need to be computed in the future work to fully investigate the ship motion coupled with LNG tank sloshing.

## Acknowledgment

This work is supported by the National Natural Science Foundation of China (51379125, 51490675, 11432009, 51579145, 11272120), Chang Jiang Scholars Program (T2014099), Program for Professor of Special Appointment (Eastern Scholar) at Shanghai Institutions of Higher Learning (2013022), Innovative Special Project of Numerical Tank of Ministry of Industry and Information Technology of China (2016-23) and Lloyd's Register Foundation for doctoral students, to which the authors are most grateful.

## Reference

- [1] Nam, B. W., Kim, Y., Kim, D. W., and Kim, Y. S. (2009). Experimental and numerical studies on ship motion responses coupled with sloshing in waves, *Journal of Ship Research* **53**(2), 68-82.
- [2] LI, Y. L., ZHU, R. C., MIAO, G. P., and Ju, F. A. N. (2012). Simulation of tank sloshing based on OpenFOAM and coupling with ship motions in time domain, *Journal of Hydrodynamics* **24**(3), 450-457.
- [3] Jiang, S. C., Teng, B., Bai, W., and Gou, Y. (2015). Numerical Simulation of Coupling Effect between Ship Motion and Liquid Sloshing under wave action, *Ocean Engineering* **108**, 140-154.
- [4] Shen, Z., and Wan, D. C. (2012). Numerical Simulations of Large-Amplitude Motions of KVLCC2 With Tank Liquid Sloshing in Waves, In *Proc 2nd Int Conf Violent Flows, Nantes, France, Ecole Centrale Nantes* (pp. 149-156).
- [5] Kim, B., and Shin, Y. S. (2008, January). Coupled seakeeping with liquid sloshing in ship tanks, In *ASME 2008 27th International Conference on Offshore Mechanics and Arctic Engineering* (pp. 247-257). American Society of Mechanical Engineers.
- [6] Mitra, S., Wang, C. Z., Reddy, J. N., and Khoo, B. C. (2012). A 3D fully coupled analysis of nonlinear sloshing and ship motion, *Ocean Engineering* **39**, 1-13.
- [7] Shen, Z., Carrica, P. M., and Wan, D. (2014, June). Ship Motions of KCS in Head Waves With Rotating Propeller Using Overset Grid Method, In *ASME 2014 33rd International Conference on Ocean, Offshore and Arctic Engineering* (pp. V002T08A043-V002T08A043). American Society of Mechanical Engineers.
- [8] Shen, Z., Wan, D., and Carrica, P. M. (2015). Dynamic overset grids in OpenFOAM with application to KCS self-propulsion and maneuvering, *Ocean Engineering* **108**, 287-306.
- [9] Dhakal, T. P., and Walters, D. K. (2009, January). Curvature and rotation sensitive variants of the K-Omega SST turbulence model, In *ASME 2009 Fluids Engineering Division Summer Meeting* (pp. 2221-2229). American Society of Mechanical Engineers.
- [10] Shen, Z., and Wan, D. (2014, August). Computation of Steady Viscous Flows around Ship with Free Surface by Overset Grids Techniques in OpenFOAM, In *The Twenty-fourth International Ocean and Polar Engineering Conference*. International Society of Offshore and Polar Engineers.
- [11] *CFD Workshop in Gothenburg 2010.* : <http://www.gothenburg2010.org>